



The recent amplifying seasonal cycle of the Arctic sea ice extent related to the subsurface cooling in the Bering Sea

Xiao-Yi Yang¹, and GuiHua Wang²

5 ¹State Key Laboratory of Marine Environmental Science, and College of Ocean and Earth Sciences, Xiamen University, Xiamen China.

²Department of Atmospheric and Oceanic Sciences & Institute of Atmospheric Sciences, Fudan University, Shanghai China

Correspondence to: Xiao-Yi Yang (xyyang@xmu.edu.cn)

Abstract. After an unprecedented and accelerated retreat, the total Arctic sea ice cover in recent decade is characterized with low extent and large amplitude of annual cycle. This study investigated the spatial-temporal variation of the Arctic sea ice extent and the potential factors accounting for its amplifying seasonal cycle. The results show that the Chukchi-Bering sector of Arctic exhibits a contrasting decadal variation of sea ice extent between the different seasons: The sea ice in recent decade decreased in summer-autumn seasons but increased significantly in spring, leading an amplifying seasonal cycle. This decadal expansion of spring Chukchi-Bering sea ice may be attributed to the significant subsurface cooling in the northern Bering Sea.

1 Introduction

The Arctic sea ice cover is an integral part of the Arctic climate system as well as one of the most effective indicators to the global climate change. Since the satellite era, the Arctic sea ice has experienced a continuous decline along with the Arctic amplification of global warming. It is noteworthy that the rate of ice loss accelerates from the late 1990s (Comiso et al., 2008; Comiso, 2012; Stroeve et al., 2012), in correspondence to the abrupt rising of Arctic surface air temperature (Screen and Simonds 2010). This is in great contrast to the simultaneous slowdown of surface warming in the Northern Hemisphere extra-polar regions (Cohen et al., 2014). Therefore the possibility of "tipping points" or abrupt changes in the Arctic climate system has come to be a subject of much debate (Lindsay and Zhang, 2005; Lenton et al., 2008; Eisenman and Wettlaufer, 2009; Armour et al., 2011; Serreze, 2011; Tietsche et al., 2011; Duarte et al., 2012; Bathiany et al., 2016a). Their controversy lies in two aspects: 1. Whether or not the Arctic sea ice cover will melt persistently and irreversibly to an ice-free state; 2. Whether or not a bifurcation with multiple steady states exists such that the Arctic may transit from perennial to seasonal ice cover. In general, the model simulation studies defied the existence of threshold or "tipping point". By modulating atmospheric carbon dioxide, Armour et al. (2011) and Bathiany et al. (2016a) demonstrated that there is neither irreversibility nor multiple states for the total Arctic sea ice cover. Tietsche et al. (2011) further proposed a recovery mechanism for Arctic summer sea ice based on the anomalous long-wave emission and atmospheric heat advection. Nevertheless, the data statistical researches presented various early warning signals for an abrupt Arctic climate change. For



example, Duarte et al. (2012) argued that it is the ice thickness rather than ice extent that cannot be rebuilt. Livina and Lenton (2013), by the "potential analysis", detected the abrupt and persistent increase in the seasonal cycle of Arctic sea ice cover since 2007.

While previous studies mostly detected the signal of abrupt Arctic climate change in terms of fast sea ice decline and the amplifying seasonal cycle, few of them noted the regional and seasonal dependence of Arctic sea ice variation. Recently, Close et al. (2015) examined the timing of onset of Arctic sea ice decline and concluded that much earlier onset time and weaker post-onset rate of loss occurred in the Pacific sector than in the Atlantic sector. This indicates that Arctic sea ice variation is asymmetrical and strongly dependent on the local physical process, resulting in the complexity and difficulty in predicting the future Arctic climate change. Therefore, we need to probe into the recent Arctic sea ice variability in detail both temporally and spatially. More urgently is to explore the physical mechanism accounting for the recent amplifying seasonal cycle of Arctic sea ice cover so as to better understand the Arctic climate change and improve the predictability of climate change.

2 Data and methods

Monthly sea ice concentration dataset from 1979 to 2015 was developed by the National Aeronautics and Space Administration team using the *Nimbus-7* SMMR (1978-87), DMSP SSM/I (1987-2009), and DMSP SSMIS (2008-present) satellite passive microwave radiances on a 25km×25km polar stereographic grid (Cavalieri et al., 2013) and can be freely downloaded from National Snow and Ice Data Center (NSIDC) website. The sea ice extent (SIE) was generated by summing the areas of the concerning grid boxes covered with at least 15% ice concentration.

The meteorological variables including surface air temperature, sea level pressure, 850hPa zonal and meridional winds, and sea surface temperature were obtained from the European Centre for Medium-Range Weather Forecasts (ECMWF) ERA-interim reanalysis dataset (Dee et al., 2011), with a horizontal resolution of 0.75°×0.75° and ranging from Jan1979 to Dec2015.

The ORAS4 ocean temperature and horizontal velocity data was used to examine the ocean subsurface variability. The ORAS4 is a newly-released version of ECMWF ocean reanalysis dataset, which is based on the NEMO ocean model and assimilates the available temperature and salinity profiles and sea-level anomalies through the NEMOVAR assimilation scheme (Balmaseda et al., 2012). The dataset spans the period of Jan1958 to Dec2015, with the resolution of 1°×1° grid horizontally and 42 levels vertically.

The monthly Pacific Decadal Oscillation (PDO) index was downloaded via JISAO website at <http://research.jisao.washington.edu/pdo/>. The NCEP Global Ocean Data Assimilation System (GODAS) data and the Hadley Centre EN4 quality controlled ocean data were also used to validate the results.



All the anomaly data was obtained by subtracting the climatological mean of 1979-1998. The running trends were estimated by applying the least square method on a moving 11-year window. The significance testing of decadal trend is at the 95% confidence level taking into account its temporal autocorrelation (Santer et al., 2000).

The amplitude of seasonal cycle is estimated by calculating the annual standard deviation based on the following formula:

$$\text{std}_j = \sqrt{\sum_{i=1}^{12} (x_{ij} - \bar{x}_j)^2}$$

where the subscripts of i, j are the month and the year, respectively. The overbar denotes the annual mean.

Zonal mean ocean temperature anomalies with PDO removed are computed by following steps: First regressing the zonal-mean temperature onto the PDO index. Then the PDO-congruent temperature anomalies are obtained by multiplying the regression coefficients with the PDO index. Finally, this PDO-congruent part is subtracted from the original zonal-mean temperature anomalies.

3 Results

3.1 Amplified seasonal cycle of the Arctic sea ice extent

The time series of monthly total Arctic SIE anomalies from Jan1979 to dec2015 is shown in Fig. 1a (upper panel), in parallel with the annual cycle magnitudes (lower panel in Fig. 1a). The total Arctic sea ice cover variability during the satellite period goes through three distinct stages: relative high extension and steadiness of sea ice cover during 1979-1998; the fast ice retreat period from 1999 to 2006; and the lower ice extension and level-off of ice retreat trend in post-2007 period. After the persistent and dramatic decline period with a rate of about -0.127 million km^2/year from 1999 to 2006, the climatology of total Arctic sea ice extent dropped down remarkably from ~ 12.2 million km^2 for the 1979-1998 period to ~ 11.3 million km^2 for the post-2007 period. In association with the slow-down of Arctic sea ice retreat is the abrupt increasing magnitude of ice fluctuation around the climatological mean in recent decade. Actually the mean value of annual standard deviation leaped from 0.25 million km^2 before 2007 up to 0.56 million km^2 after the year of 2007. Therefore, the Arctic sea ice in recent decade is characterized by the lower coverage, the level-off linear trend and the intensive seasonal fluctuation. All these signals herald the transition of Arctic climate regime, which is one of the hot topics in climate research community (Livina and Lenton 2013; Bathiany et al., 2016b)

In view of the strong seasonality and localization of Arctic sea ice variability, we further probed into the fine structure of ice regime shift by contrasting the differences of meridional ice extent between the 2007-2015 mean and the 1979-1998 mean in a month-longitude section (Fig. 1b). The Atlantic sector including Baffin Bay, Greenland Sea and Barents and Kara seas exhibits uniform and season-independent descents of sea ice extent. In contrast, the sea ice extent in the Pacific sector decreased in summer-fall season but increased in winter-spring season in recent decade. This seasonality is extraordinarily evident in the Chukchi-Bering (ChukBer) seas, where the SIE annual standard deviation goes through a sharp rise of ~ 0.24



million sq. km in the last decade by reference to the period of 1979-1998. The seasonality of the ChukBer SIE mean state change as shown in figure 1b recurs on the decadal time scale. The 10-yr running trend analysis of ChukBer SIE reveals the notable retreat in August-October and expansion in March-May since the early 2000s (Fig. 1c). The strong contrast of SIE decadal trends in the ChukBer region is partially offset by the uniformly accelerated ice retreat around the whole year in the Atlantic sector (Figure not shown), contributing to the recent amplifying seasonal cycle of total Arctic sea ice.

It is widely recognized that significant summertime ice loss in the Chukchi Sea is primarily attributed to ice-albedo positive feedback thermodynamically and strengthening transpolar drift dynamically. So far there is a lack of comprehensive understanding and interpretation for the recent expansion of ChukBer ice extent in spring, which is critical to intensification of Arctic sea ice annual cycle. Therefore, we constructed the normalized spring (March-May mean) ChukBer Sea ice extent index (SBII) as shown in Fig. 1d. Based on the threshold of ± 1 standard deviation of SBII, a total of 15 out of 37 years are selected to do the following composite analysis, including 8 high index years (1984, 1994, 1999, 2008, 2009, 2010, 2012 and 2013) and 7 low index years (1979, 1989, 1996, 2002, 2003, 2004, 2015).

3.2 Abrupt transition of air-sea interaction in the Pacific sector

To interpret the abrupt change of total Arctic SIE prior- and post-2007 in terms of the climate change in the Bering Sea, various related physical variables are composited based on SBII index (high index years minus low index years) in two periods of 1979-2006 (Fig. 2 left panels) and 2007-2015 (Fig. 2 right panels). For both periods, the anomalous expansion of SBII corresponds to the significant cooling (negative anomalies of surface air temperature) over the Bering area (Fig. 2a & d). However, the surface heat flux, SLP and 850hPa wind anomalies associated with the SBII present completely different patterns for the two periods. In 1979-2006, the Chukchi-Bering region is dominated by the anomalous SLP dipole pattern and the attendant northerly winds in the lower troposphere (Fig. 2b). The local air temperature drops accordingly, leading to intense heat loss over a broad area of north Pacific high latitudes (Fig. 2c). In contrast to the early period, the spring Bering Sea ice expansion after 2007 is associated with an insignificant high SLP anomaly and the patchy northerly winds on its eastern flank (Fig. 2e). There is no apparent oceanic heat loss but significant reverse heat transfer from atmosphere to ocean over the ice-covered northern Bering Sea (Fig. 2f). We therefore speculated that the Bering Sea surface cooling rather than the overlying atmospheric process may be responsible for the spring ice cover expansion in recent decade.

To further verify the correspondence of SBII and the Bering Sea surface temperature, we compared the composite patterns of North Pacific SST anomalies on the SBII between the two periods (Fig. 3a). The positive SBII phase is associated with the local surface cooling confined in the Bering Sea area for the early period. In the later period, however, the spring Bering sea ice expansion is connected to a large-scale SST anomaly pattern similar to Pacific Decadal Oscillation (PDO) mode, i.e., the significant cooling in the Bering Sea can extend along the costal North America to the central tropical Pacific, sandwiching the warming anomalies in the adjacent area of the Kuroshio extension (Fig.3b). We then examined the monthly PDO index and found the obvious phase shift from positive PDO to negative PDO in 2000s (Fig. 4). Many studies already



noticed this Pacific climate regime shift and its connection with the recent global warming hiatus (Trenberth and Fasullo 2013; England et al., 2014). The time series of the spring (March-May mean) PDO index and the SBII are shown in Fig. 3c. There is significant negative correlation between the two indices, with the correlation coefficient of -0.47 during the whole period. Echoing the transition of North Pacific climate, an obvious decadal change appears in the correlation between the
5 PDO and SBII. The correlation coefficient leaps up over -0.7 in the new century, in great contrast to zero correlation in the early two decades. The month-by-month correlation of PDO with SBII reveals that in the inter-annual time scale, the SBII lead PDO by 0~6 months (Fig. 3d). This to some extent rules out the possibility that the recent Bering Sea cooling is directly triggered by the Pacific climate regime shift. In other words, the Bering Sea cooling may coincide with the recent phase switch of PDO.

10

3.3 Subsurface cooling of the Bering Sea in recent decade

To explore the mechanism that is responsible for recent ocean-dominant ice variation, we composite the Bering Sea zonal-mean (160 °-200 °E mean) temperature anomalies (with PDO removed) based on the SBII high minus low index for the two periods, as shown in Fig. 5 a & b. In the early period, the expansion of spring Bering ice cover corresponds to the
15 significant cooling in the upper ocean extending from sea surface to the subsurface layer at the southern flank of Bering Strait (Fig. 5a). The significant subsurface cooling reappears in recent decade with its maxima centered in 100-300m, but the surface cooling is insignificant (Fig. 5b). This further underlines the ocean role in facilitating the increase of Bering Sea ice area. The 11-year running trends of ocean temperature in the Bering Sea area (160 °-200 °E, 55 °-65 °N mean) are displayed in Fig. 5c. It is as expected that the remarkable cooling trends emerge after ~2007, with the maximum at subsurface layer of
20 ~165m.

To validate this result, we compared the time series of 3 month running mean temperature at 165m from the ORAs4 data with those from the GODAS and HadEN4 datasets (Fig. 6). All three datasets agree on the abrupt descent of subsurface temperature in recent decade, in spite of the discrepancies in their transition time and amplitude within limits. In particular, the ORAs4 temperature shows the greatest drop of ~0.8°C in the time of 2007. The HadEN4 data is consistent with the
25 ORAs4 in transition time but in smaller amplitude, while the transition time of GODAS temperature is two year earlier than the other two datasets.

What triggered the abrupt drop of temperature in the Bering Sea upper ocean after 2007? Fig. 5d shows the climatological change of temperature and ocean circulation in subsurface Bering Sea at 165m for the prior- and post- 2007 periods. The recent subsurface cooling in Bering Sea corresponds to an anomalous anticyclone circulation in the Bering Sea.
30 The climatological circulation in Bering Sea is characterized by a cyclonic gyre, composed of a strong western boundary cold current (i.e., East Kamchatka Current) and a weak and warm Alaska stream (figure not shown). This anomalous anticyclone circulation is associated with the dramatic decrease of the warm advection by the Alaska stream, which may lead to the cooling in the Bering Sea. Another possible factor accounting for the Bering Sea cooling is the local wind stress. There



is an anomalous high pressure and correspondingly anticyclonic atmosphere circulation over the Bering Sea in recent decade (Fig. 7). The anomalous southwestlies over the northwest of Bering Sea tend to induce the coastal upwelling of colder deep water along the coast, thereby facilitates the cooling in the northern Bering Sea. More detailed diagnostics and analysis are required to ascertain the dynamical processes for the recent subsurface cooling in the Bering Sea.

5

4 Conclusions and discussion

By dissecting spatial-temporal variability of the Arctic sea ice, this study investigated the physical mechanism that accounts for the amplifying seasonal cycle of total Arctic SIE in recent decade. The key point accounting for the increased amplitude of seasonal cycle lies in the Bering Sea, where the sea ice cover expands due to the significant subsurface cooling in recent decade. This, in great contrast to the continuous surface warming in the pan-Arctic region, may shed light on the future Arctic climate change.

Woodgate et al. (2010) reported the increasing oceanic heat flux over the Bering Strait since the early 2000s, and proposed that this Bering Strait inflow may act as a conduit for oceanic heat into the Arctic and contribute to the unprecedented seasonal Arctic sea-ice loss in 2007. Echoing to this increasing heat flux into the Arctic Ocean, the Bering Sea is reported to be the only substantial non-coastal area with lengthening sea ice seasons within the Pan-Arctic region (Parkinson, 2014). Our result is generally consistent with these previous studies: The increasing oceanic heat flux over the strait may lead to anomalous warming in the central Arctic Ocean and cooling in the Bering Sea, therefore the seasonal contrast of sea ice variability in the Pacific sector and the lengthening sea ice season in the Bering Sea. By the preliminary analysis, we go further to propose that the decadal change of local oceanic and atmospheric circulation change, i.e., the anomalous oceanic temperature advection and/or the coastal upwelling may account for the abrupt subsurface cooling in the Bering Sea after 2007.

In addition to local dynamical processes, previous studies also demonstrated that the Chukchi-Bering climate variability for the post-1999 period is closely related to Pacific basin-scale atmospheric and oceanic circulation patterns, e.g., the North Pacific Oscillation (NPO), the North Pacific Gyre Oscillation (NPGO) as well as the central Pacific El Nino (Yeo et al., 2014). Indeed, the SBII time series in Fig. 1d exhibits an obvious change in its period. The SBII varied mainly in the interannual time scale before 2000, and after that in decadal time scale, coinciding with the NPO-NPGO couple mode in 1999-2010. In this sense, the abrupt Arctic sea ice cover change may also connect to the Pacific climate regime shift. Therefore, further study is necessary to undermine the leading player in the recent Arctic climate change. In order to answer the questions like whether this tendency of amplifying seasonal cycle of Arctic sea ice cover will sustained or not and whether it will lead to the nonlinear instability of the Arctic climate system, we should improve our understanding on the Bering Sea thermal state and dynamical processes as well as its connection to the North Pacific climate mode.

30

Acknowledgments



We thank ECMWF for providing the reanalysis datasets of ERAinterim and ORA-s4, and NSIDC for providing the sea ice concentration dataset.

X.-Y. Yang is supported by the Natural Science Foundation of China (Grant 41576178). G. Wang is supported by the Natural Science Foundation of China (91428206, 91528304), the National Program on Global Change and Air-Sea
5 Interaction (GASIIPOVAI-04) and Program Of Shanghai Academic Leader (17XD1400600).

References

- Armour, K. C., Eisenmann, I., Blanchard-Wrigglesworth, E., McCusker, K. E., and Bitz, C. M.: The reversibility of sea ice
10 loss in a state-of-the-art climate model, *Geophys. Res. Lett.*, 38, L16705, doi: 10.1029/2011GL048739, 2011.
- Balmaseda, M. A., Mogensen, K., and Weaver, A. T.: Evaluation of the ECMWF ocean reanalysis system ORAS4, *Q. J. Roy. Meteor. Soc.*, 139, 1132-1161, doi: 10.1002/qj.2063, 2012.
- Bathiany, S., Notz, D., Mauritsen, T., Raedel, G., and Brovkin, V.: On the potential for abrupt Arctic winter sea ice loss, *J. Clim.*, 29, 2703-2719, doi: 10.1175/JCLI-D-15-0466.1, 2016a.
- 15 Bathiany, S., Bolt, B. van der, Williamson, M. S., Lenton, T. M., Scheffer, M., Nes, E. van, and Notz, D.: Trends in sea-ice variability on the way to an ice-free Arctic, *The Cryosphere Discussions*, doi: 10.5194/tc-2015-209, 2016b.
- Cavaliere, D. J., Parkinson, C. L., Gloersen, P., and Zwally, H. J.: Sea ice concentrations from *Nimbus-7* SMMR and DMSP SSM/I-SSMIS passive microwave data, version 1 [dataset], National Snow and Ice Data Center, accessed March 2014, Available online at <http://nsidc.org/data/nsidc-0051.html>, 2013.
- 20 Close, S., Houssais, M. –N., and Herbaut, C.: Regional dependence in the timing of onset of rapid decline in Arctic sea ice concentration, *J. Geophys. Res.*, 120(12), 8077-8098, doi: 10.1002/2015JC011187, 2015.
- Cohen, J., Screen, J. A., Furtado, J. C., Barlow, M., Whittleston, D., Coumou, D., Francis, J., Dethloff, K., Entekhabi, D., Overland, J., and Jones, J.: Recent Arctic amplification and extreme mid-latitude weather, *Nature Geosci.*, 7, 627-637, doi: 10.1038/NGEO2234, 2014.
- 25 Comiso, J. C., Parkinson, C. L., Gersten, R., and Stock, L.: Accelerated decline in the Arctic sea ice cover, *Geophys. Res. Lett.*, 35, L01703, doi:10.1029/2007GL031972, 2008.
- Comiso, J. C.: Large decadal decline of the Arctic multiyear ice cover, *J. Clim.*, 25, 1176-1193, 2012.
- Dee, D. P., and coauthors: The ERA-Interim reanalysis: Configuration and performance of the data assimilation system, *Q. J. Roy. Meteor. Soc.*, 137, 553-597, doi: 10.1002/qj.828, 2011.
- 30 Duarte, C. M., Lenton, T. M., Wadhams, P., and Wassmann, P.: Abrupt climate change in the Arctic, *Nature Climate Change*, 2, 60-62, 2012.



- Eisenman, I., and Wettlaufer, J. S.: Nonlinear threshold behavior during the loss of Arctic sea ice, *PNAS*, 106(1), 28-32, doi: 10.1073/pnas.0806887106, 2009.
- England, M. H., and coauthors: Recent intensification of wind-driven circulation in the Pacific and the ongoing warming hiatus, *Nature Climate Change*, 4, 222-227, doi: 10.1038/NCLIMATE2106, 2014.
- 5 Lenton, T. M., Held, H., Kriegler, E., Hall, J. W., Lucht, W., Rahmstorf, S., and Schellnhuber, H. J.: Tipping elements in the Earth's climate system, *PNAS*, 105(6), 1786-1793, doi: 10.1073/pnas.0705414105, 2008.
- Lindsay, R. W., and Zhang, J.: The thinning of Arctic sea ice, 1988-2003: Have we passed a tipping point? *J. Clim.*, 18, 4879-4894, 2005.
- Livina, V. N., & Lenton, T. M.: A recent tipping point in the Arctic sea-ice cover: abrupt and persistent increase in the seasonal cycle since 2007, *The Cryosphere*, 7, 275-286, doi: 10.5194/tc-7-275-2013, 2013.
- 10 Parkinson, C. L.: Spatially mapped reductions in the length of the Arctic sea ice season, *Geophys. Res. Lett.*, 41, 4316-4322, doi: 10.1002/2014GL060434, 2014.
- Pinker, R. T., Niu, X., and Ma, Y.: Solar heating of the Arctic Ocean in the context of ice-albedo feedback, *J. Geophys. Res.: Oceans*, 119, 8395-8409, doi: 10.1002/2014JC010232, 2014.
- 15 Santer, B. D., Wigley, T. M. L., Boyle, J. S., Gaffen, D. J., Hnilo, J. J., Nychka, D., Parker, D. E., and Taylor, K. E.: Statistical significance of trends and trend differences in layer-average atmospheric temperature time series, *J. Geophys. Res.*, 105(D6), 7337-7356, 2000.
- Screen, J. A., and Simmonds, I.: The central role of diminishing sea ice in recent Arctic temperature amplification, *Nature*, 464, 1334-1337, doi: 10.1038/nature09051, 2010.
- 20 Serreze, M. C., Barrett, A. P., Stroeve, J. C., Kindig, D. N., and Holland, M. M.: The emergence of surface-based Arctic amplification, *The Cryosphere*, 3, 11-19, 2009.
- Serreze, M. C.: Rethinking the sea-ice tipping point, *Nature Climate Change*, 471, 47-48, 2011.
- Stroeve, J. C., Serreze, M. C., Holland, M. M., Kay, J. E., Malanik, J., and Barrett, A. P.: The Arctic's rapidly shrinking sea ice cover: a research synthesis, *Climate Change*, 110, 1005-1027, doi: 10.1007/s10584-011-0101-1, 2012.
- 25 Tietsche, S., Notz, D., Jungclauss, J. H., and Marotzke, J.: Recovery mechanism of Arctic summer sea ice, *Geophys. Res. Lett.*, 38, L02707, doi: 10.1029/2010GL045698, 2011.
- Trenberth, K. E., and Fasullo, J. T.: An apparent hiatus in global warming? *Earth's Future*, 1, 19-32, doi: 10.1002/2013EF000165, 2013.
- Woodgate, R. A., Weingartner, T., and Lindsay, R.: The 2007 Bering Strait oceanic heat flux and anomalous Arctic sea-ice retreat. *Geophys. Res. Lett.*, 37, L01602, doi: 10.1029/2009GL041621, 2010.
- 30 Yeo, S.-R., Kim, K.-Y., Yeh, S.-W., Kim, B.-M., Shim, T., and Jhun, J.-G.: Recent climate variation in the Bering and Chukchi Seas and its linkages to large-scale circulation in the Pacific. *Climate Dynamics*, 42, 2423-2437, doi: 10.1007/s00382-013-2042-z, 2014.

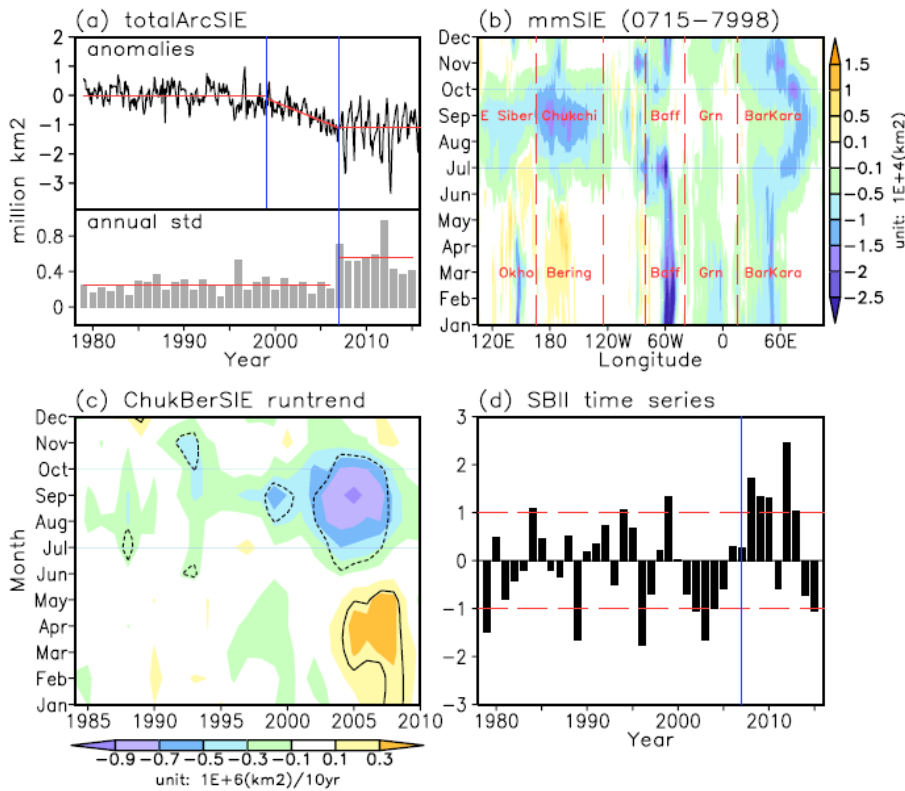


Figure 1: (a) Time series of total Arctic sea ice extent anomalies (upper panel) and annual standard deviation (lower panel) during the period of 1979-2015. Red lines denote the mean values and the linear trend slope for different period. 5 Vertical blue lines indicate the critical years of 1999 and 2007 for the abrupt change of Arctic sea ice cover. (b) Seasonality of sea ice extent climatologic change (2007-2015 mean minus 1979-1998 mean) for each longitude (the red dashed lines roughly demarcate the different sectors of the Arctic marginal seas). (c) Decadal running trends of the Chukchi-Bering sea ice extent for each month. Trends are centered on the indicated year (e.g. the trend at 1985 is based on data from 1980 to 1990). Solid (dashed) lines encircle the positive (negative) trends that exceed the 95% 10 confidence level. (d) Time series of normalized spring (March-May mean) Bering sea ice extent (SBII). Red dashed lines indicate the threshold of ± 1 standard deviation for selecting the composite years. Vertical blue line indicates the critical year of 2007.

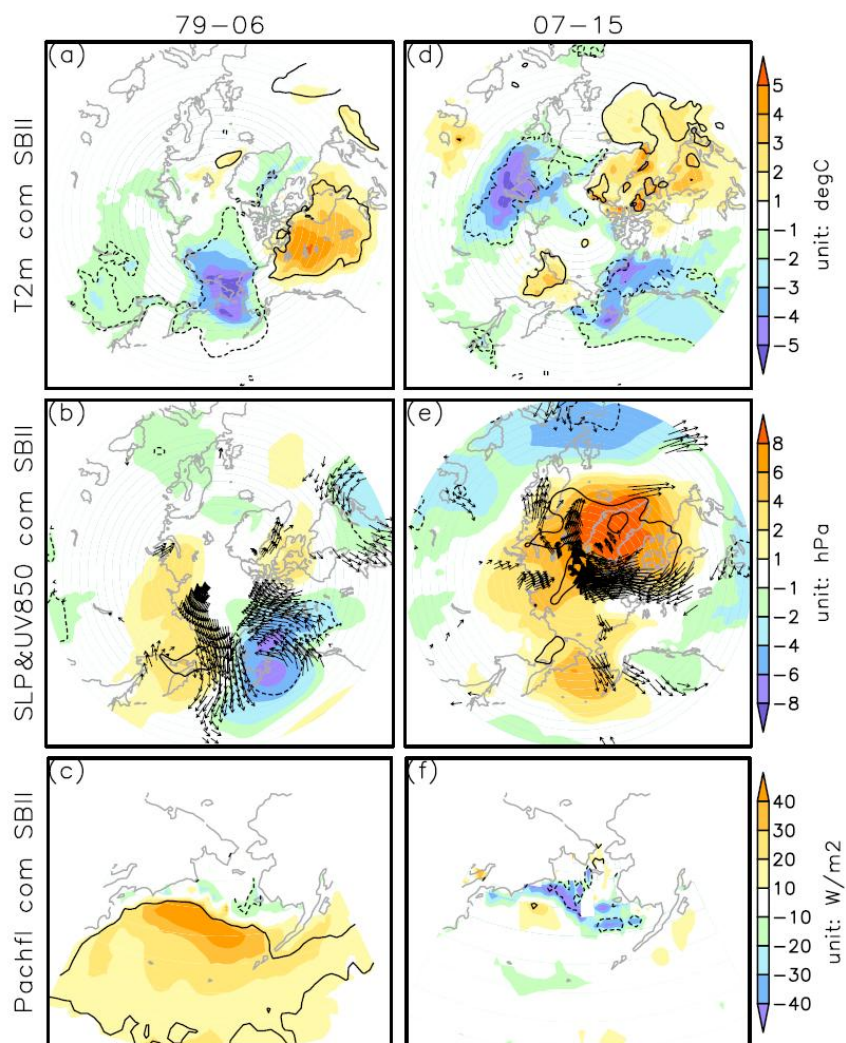


Figure 2. Composites of (a)&(d) 2-metre air temperature anomalies; (b)&(e) sea level pressure (color shading) and 850hPa wind (vectors) anomalies; and (c)&(f) North Pacific turbulent surface heat flux (sensible plus latent heat) anomalies based on SBII high minus low index during the prior-2007 period (left panels) and the post-2007 period.

5 Solid (dashed) lines enclose the positive (negative) values that are significant at the 95% confidence level. For 850hPa wind vectors, only the zonal or meridional wind anomalies that significant at 95% confidence level are displayed.

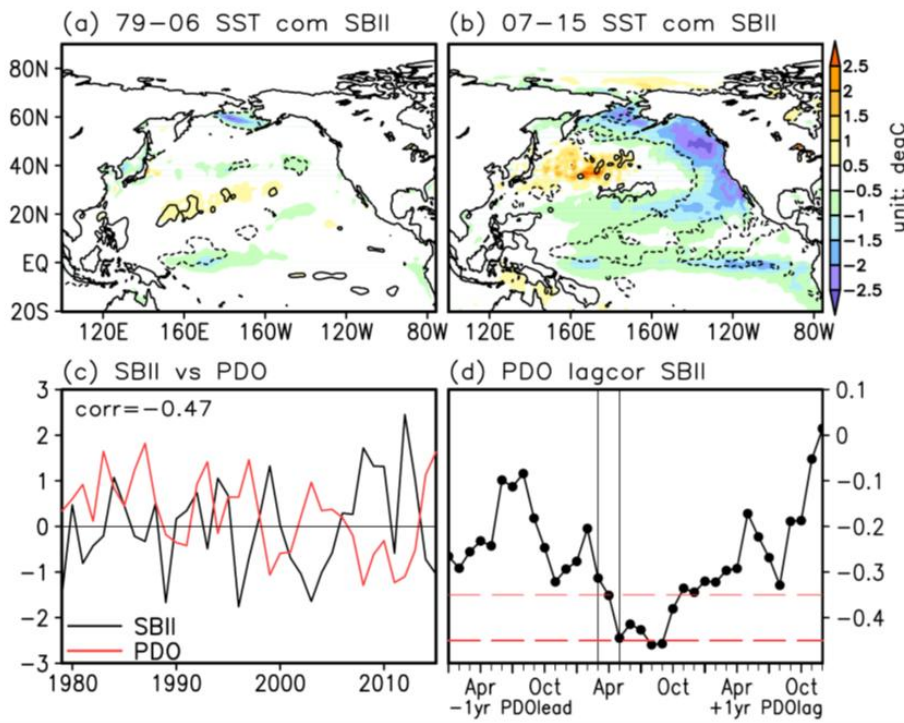


Figure 3. (a) Composite of spring (March-May mean) sea surface temperature anomalies based on SBII during the period of 1979-2006. Solid (dashed) lines enclose the positive (negative) values that are significant at the 95% confidence level. (b) Same as (a), but composite during the period of 2007-2015. (c) Time series of SBII (black) and annual mean PDO index (red). (d) Lead-lag correlation coefficients between the monthly PDO index and SBII. Thin (thick) dashed red lines indicate the 95% (99%) confidence level. Two solid black lines designate the months of March-May, when PDO correlates SBII with zero time lag.

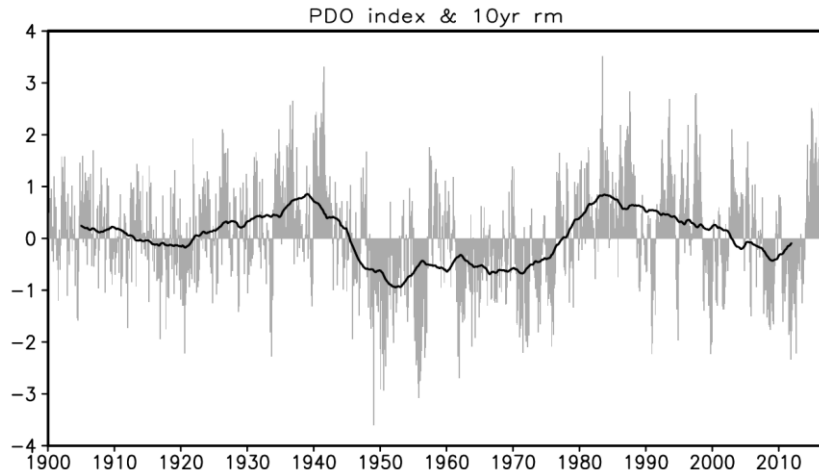
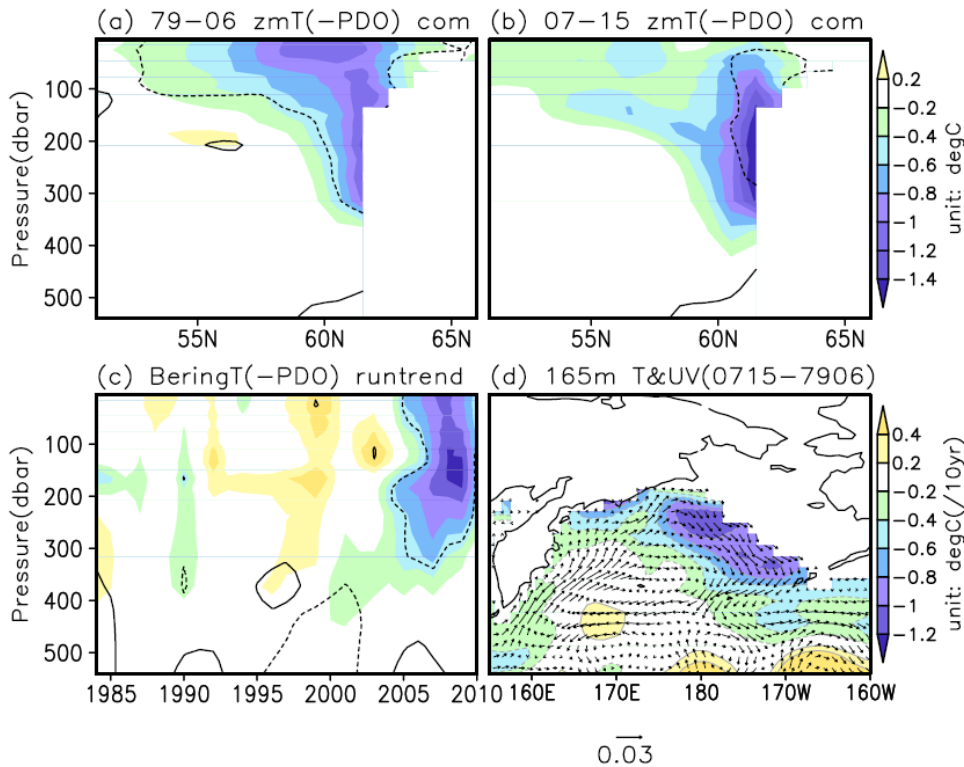


Figure 4. Monthly PDO index (gray bars), superposing its decadal component (120-month running mean, thick black line)



5

Figure 5. (a) 1979-2006 composites of spring (March-May mean) zonal-mean temperature anomalies (with the PDO-congruent part subtracted from the original data) based on SBII. Solid (dashed) lines enclose the positive (negative)



values that are significant at the 95% confidence level. (b) Same as (a), but composites for the period of 2007-2015. (c) 11 year running trends of spring Bering Sea temperature (with the PDO-congruent part subtracted from the original data). Solid (dashed) lines enclose the positive (negative) trends that are significant at the 95% confidence level. (d) Decadal change of temperature (color shading) and horizontal velocity at 165m level with the 2007-2015 mean minus 1979-2006 mean. (c) and (d) share the same color bar with different units, i.e., degC/10yr for (c) and degC for (d).

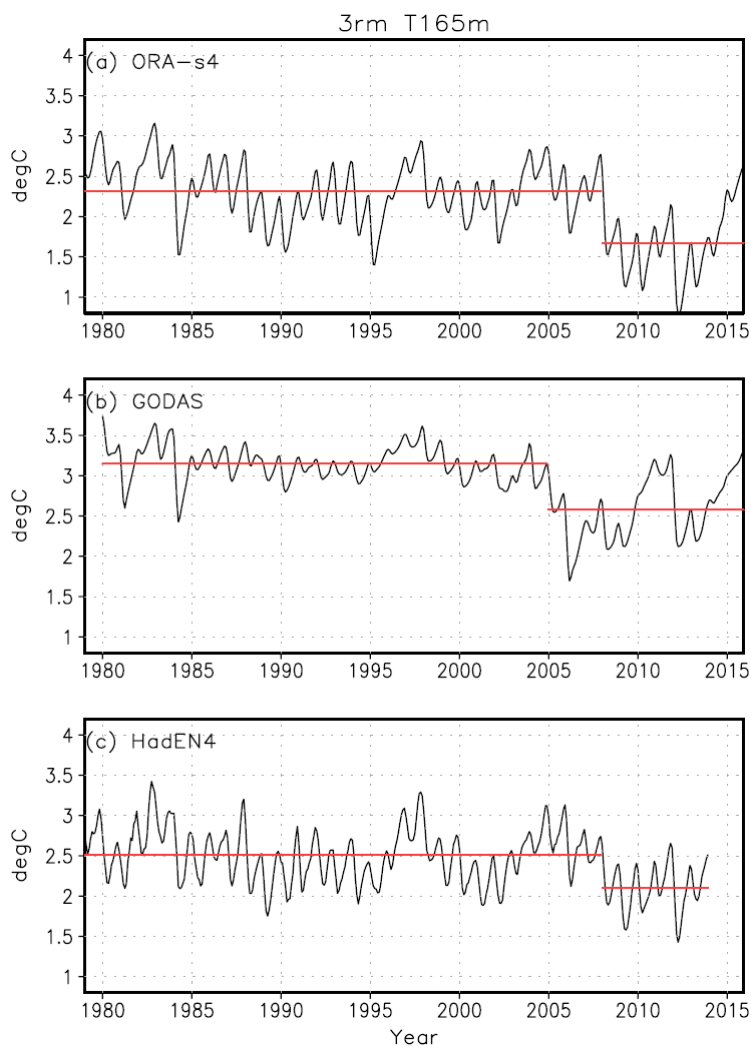


Figure 6. (a) ORA-s4 time series of 3-month running mean subsurface temperature at about 165m depth. The red lines indicate the means for the period of prior- and post- 2007. (b) Same as (a), but for the GODAS dataset. The red lines indicate the means for the period of prior- and post- 2005. (c) Same as (a), but for the HadEN4 dataset.

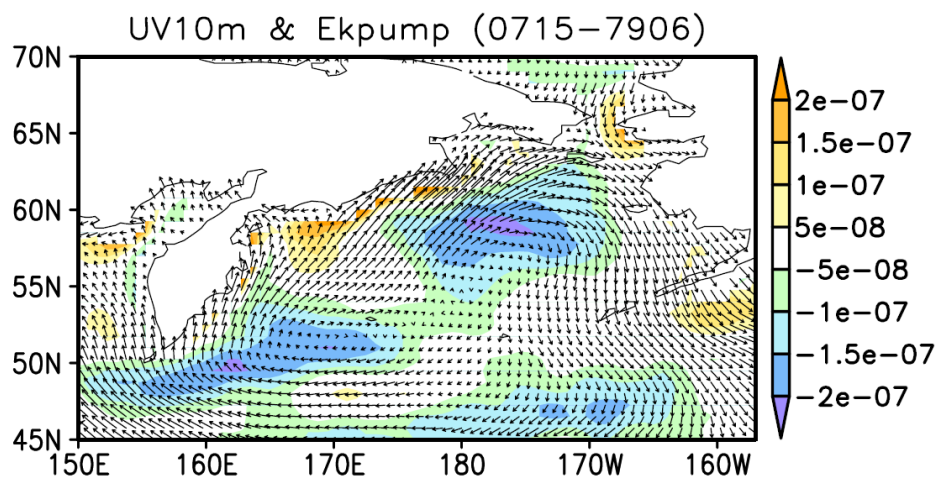


Figure 7. Decadal change of Ekman pumping rate (color shading) and 10m U, V wind (vectors) with the 2007-2015 mean minus 1979-2006 mean.